Solvent Drag across Gramicidin Channels Demonstrated by Microelectrodes

Peter Pohl and Sapar M. Saparov
Martin-Luther-Universität, Medizinische Fakultät, Institut für Medizinische Physik und Biophysik, 06097 Halle, Germany

ABSTRACT The competition of ion and water fluxes across gramicidin channels was assessed from the concentration distributions of both pore-impermeable and -permeable cations that were simultaneously measured by double-barreled microelectrodes in the immediate vicinity of a planar bilayer. Because water movement across the membrane led to accumulation of solutes on one side of the membrane and depletion on the other, the permeable cation was not only pushed by water across the channel (true solvent drag); it also flowed along its concentration gradient (pseudo-solvent drag). For the demonstration of true solvent drag, a difference between the bulk concentrations on the hypertonic and the hypotonic sides of the membrane was established. It was adjusted to get equal cation concentrations at both membrane/water interfaces. From the sodium and potassium fluxes measured along with membrane conductivity under these conditions, approximately five water molecules were found to be transported simultaneously with one ion through the channel. In diphytanoyl phosphatidylcholine membranes, a single-channel hydraulic permeability coefficient of 1.6×10^{-14} cm^3 s^{-1} was obtained.

INTRODUCTION

Passive water movement across biological membranes occurs via different pathways: by a solubility-diffusion mechanism across the lipid matrix (Hanai and Haydon, 1966), across transient defects arising from density fluctuations in the bilayers (Deamer and Bramhall, 1986; Jansen and Blume, 1995), and across permanent aqueous pores (Hill, 1995). In the latter case the solvent flux should be coupled to the flux of a solute that is also permeant through the transmembrane channels. During osmosis, for example, the solute is pushed through pores by the solvent, i.e., the solute flux is increased in the direction of water flow and is retarded in the opposite direction (Fig. 1 *d*). This phenomenon is called true solvent drag.

Because coupling of solute and solvent fluxes cannot occur via the solubility diffusion mechanism, solvent drag studies have been widely used to establish a porous transport pathway (Rippe and Haraldsson, 1994). From this kind of experiments it was suggested, for example, that the passage for nonelectrolytes may be a water transport pathway in salivary epithelium (Nakahari et al., 1996). The hamster low-density lipoprotein is sieved by the solvent through pores of the endothelial barrier in perfused mesentery microvessels (Rutledge et al., 1995). Paracellular intestinal adsorption of nutrients is realized by solvent drag (Pappenheimer et al., 1994) and is driven at least in part by their own concentration gradients. Potassium reabsorption in the proximal tubule of the rat is mediated by both solvent drag and K^+ diffusion along an existing concentration gradient. It is extremely difficult, however, to resolve their contributions (Wilson et al., 1997).

An experimentally observed increase in transmembrane solute flux that accompanies water flow does not necessarily mean that true solvent drag is involved, because there is a solute concentration gradient, Δc, across the membrane that causes a solute flux, $J_{m,p}$, in the same direction as the water flux, J_w (Fig. 1 *b*). Origin of the solute concentration gradient is the osmotic flow, i.e., water that passes through the membrane dilutes the solution it enters and concentrates the solution it leaves (Fettiplace and Haydon, 1980). These concentration changes may be restricted to the so-called unstirred layers (USLs) adjacent to the membrane that are present even in vigorously stirred systems. Δc gives rise to a solute flux that masquerades as solvent drag and is, therefore, named pseudo-solvent drag (Barry and Diamond, 1984). In addition, within the USLs the osmolyte is also diluted. As a consequence, the steady-state flow rate tends to be less than the value that would be obtained in the absence of USL effects.

A true solvent drag effect is very difficult to demonstrate, even in such a well-defined system as that represented by planar bilayers. The only published attempt was carried out with amphotericin-treated membranes (Andreoli et al., 1971). Because the evidence presented in favor of the predicted solvent drag effect was rather indirect, their experiment was criticized as unconvincing (Finkelstein, 1987). The visualization of true solvent drag requires the polarization effects within USLs to be considered. With potential measurements in the presence of valinomycin, an estimate for differences in interfacial local salt concentrations caused by water movement across the lipid bilayer may be obtained (Rosenberg and Finkelstein, 1978a). While valid in the streaming potential measurements, the valinomycin technique cannot be extended for use with high gramicidin concentrations and hence cannot be used in solvent drag experiments. Additional polarization effects are induced by

Received for publication 1 November 1999 and in final form 4 February 2000.

Address reprint requests to Dr. Peter Pohl, Institute of Medical Physics and Biophysics, Halle-Wittenberg, Medical Department, Martin-Luther University, 06097 Halle, Germany. Tel.: 49-345-5571243; Fax: 49-345-5571632; E-mail: peter.pohl@medizin.uni-halle.de.

0006-3495/00/05/2426/09 $2.00

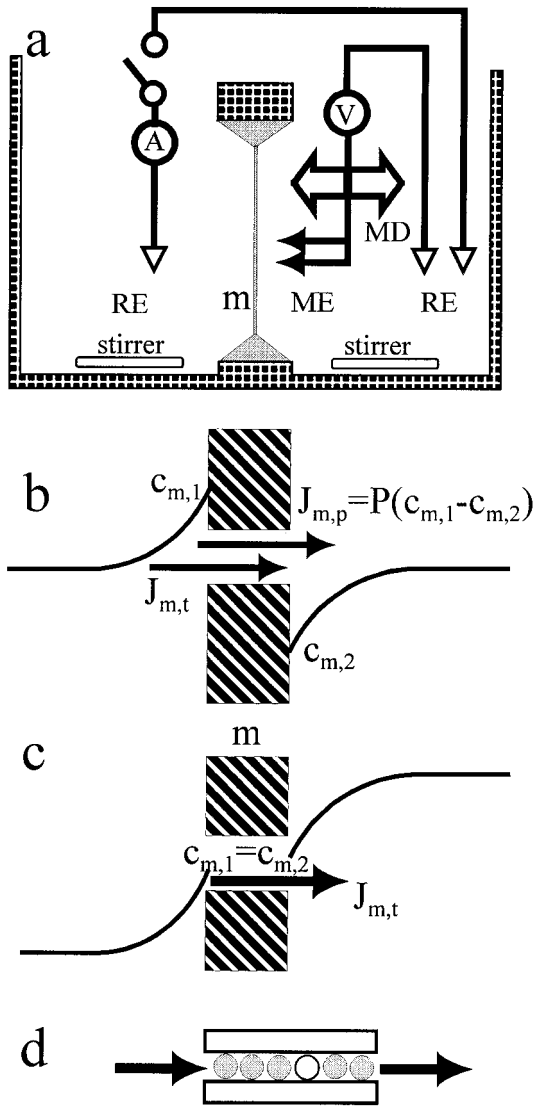

FIGURE 1 (*a*) In the immediate vicinity of a planar lipid bilayer (m), the spatial distributions of two different ions were monitored simultaneously. Therefore, a double-barreled microelectrode (ME) and a reference electrode (RE) were placed on the *trans* side of the membrane. The cation-sensitive microelectrode was moved perpendicularly to the membrane surface by a hydraulic microdrive manipulator (MD). Under short-circuited conditions, the current between two reference electrodes immersed in the buffer solutions on the two sides of the membrane was measured with a picoampermeter. The bulk solutions were stirred permanently. (*b*) Because water movement across the membrane led to accumulation of solutes on one side of the membrane (near-membrane concentration, $c_{m,1}$) and depletion on the other (near-membrane concentration, $c_{m,2}$), the permeable cation was not only pushed by water across the channel (true solvent drag, $J_{m,t}$); it also flowed along its concentration gradient (pseudo-solvent drag, $J_{m,p}$). $J_{m,p}$ is proportional to the solute membrane permeability (P) and the transmembrane concentration difference. (*c*) For the demonstration of true solvent drag, a difference in the bulk concentrations on the hypertonic and hypotonic sides of the membrane was established such that the cation concentrations at the two membrane/water interfaces were equal to each other. Under these conditions $J_{m,p}$ is zero. (*d*) During osmosis, the solute (○) is pushed through pores by the solvent (●), i.e., the solute flux is increased in the direction of water flow (→) and is retarded in the opposite direction. This phenomenon is called true solvent drag.

volume flow across a large number of water-conducting channels. We have shown that Δc in the presence and in the absence of channels may differ by an order of magnitude in the extreme case.

The use of ion-selective microelectrodes instead of valinomycin to assess the concentration changes in USLs was introduced independently by Pohl et al. (1997) and Tripathi and Hladky (1998). Whereas the former used the microelectrode technique to calculate both the water flux (Pohl et al., 1997) and the ion flux densities (Antonenko et al., 1993, 1997), the latter were the first to employ this method to monitor streaming potentials. If the measured potentials are true streaming potentials, then a genuine solvent drag effect must exist.

The present paper confirms experimentally that the effect is present; i.e., the osmotic water flow is shown to push cations across gramicidin channels in the absence of a transmembrane ion concentration difference. Solvent drag visualization was achieved by simultaneous measurements of the near-membrane concentration distributions of an impermeable and a permeable solute. The number of water molecules, N, transported per sodium and potassium ion that is obtained from solvent drag measurements is consistent with that determined via electroosmosis (Levitt et al., 1978; Rosenberg and Finkelstein, 1978b) and streaming potential (Rosenberg and Finkelstein, 1978b; Levitt, 1984; Tripathi and Hladky, 1998) measurements.

THEORY

Water and ion flow across membranes can significantly perturb nonelectrolyte and electrolyte concentrations in the USLs. The thickness of the USL, δ, is determined in terms of the concentration gradient at the interface (Dainty, 1963):

$$\frac{|c_s - c_b|}{\delta} = \left.\frac{\partial c}{\partial x}\right|_{x=0}, \tag{1}$$

where x, c_b, and c_s denote the distance from the membrane and the solute concentrations in the bulk and at the surface ($x = 0$), respectively.

The flux of ions across the membrane, J_m, is equal to their flux through the USLs. Within the USLs, the osmotic advection is countered by both back-diffusion and stirring (Pedley, 1983). According to the model of stagnant point flow (Schlichting and Gersten, 1997), it is assumed that the stirring velocity perpendicular to the membrane is equal to the product of the stirring parameter, a, and the square of the distance, x, to the membrane. The superposition of diffusion, water flow, and convection is described by the following equation (Pohl et al., 1997):

$$J_m = D\,dc/dx + (v_t - ax^2)c, \tag{2}$$

where c, D, and v_t are the concentration of the solute, its diffusion coefficient, and the velocity of transmembrane

water flow. Equation 2 may be applied only within the USL ($x < \delta$), where $v_t > ax^2$. It has been solved for the case of an impermeable solute, which implies that J_m is zero (Pohl et al., 1997). The concentration course of an impermeable solute, $c_i(x)$, is equal to

$$c_i(x) = c_{i,s}e^{-(v_t x/D_i)+(ax^3/3D_i)}, \quad (3)$$

where $c_{i,s}$ and D_i are the surface concentration and the diffusion coefficient of the impermeant solute, respectively.

Although obtained for unmodified bilayers, Eq. 3 holds also for gramicidin-containing bilayer membranes that are explored under open-circuited conditions. In this situation, the near-membrane concentration shifts are caused solely by water flow. There can be no net ion transport across membrane channels, because charge would accumulate in one compartment (Dani and Levitt, 1981). Osmosis occurs mainly across gramicidin channels that are not occupied by ions, because cations and water molecules cannot pass each other within the channel, i.e., the transport of ions and water across these channels is by a single-file process (Levitt et al., 1978; Finkelstein and Andersen, 1981). Because of the incorporation of cation-selective channels, the hydraulic membrane conductivity, P_f, increases. It can be represented as the sum of the water permeability of the lipid bilayer, $P_{f,l}$, and the channel water permeability, $P_{f,c}$:

$$P_f = (P_{f,l} + P_{f,c}) = \frac{v_t}{\chi c_{osm} V_w}, \quad (4)$$

where V_w, χ, and c_{osm} are, respectively, the partial molar volume of water, the osmotic coefficient (0.93 for urea), and the near-membrane concentration of the solute used to establish the transmembrane osmotic pressure difference. In the same way, a lipid and a channel component of the velocity, v_l and Δv, respectively, of water flow may be distinguished:

$$v_t = v_l + \Delta v$$

$$\text{with } v_l = P_{f,l}\chi c_{osm} V_w \quad \text{and} \quad \Delta v = P_{f,c}\chi c_{osm} V_w. \quad (5)$$

Δv reflects the increase in water flow velocity observed after gramicidin channel insertion into the bilayer. It is equal to the velocity of water flow through the channels multiplied by the fraction of membrane cross-sectional area represented by channels. It is assumed that there are no inhomogeneities of the fluid velocity because the gramicidin channels are narrow pores, and they tend to aggregate only at a very high peptide/lipid ratio (Ge and Freed, 1999).

The sum of v_l and Δv is related to the water flux J_w that can be calculated according to (Barry and Diamond, 1984)

$$J_W = v_t/V_W. \quad (6)$$

If a gramicidin-containing membrane is explored under short-circuited conditions, J_m is different from zero. In this case Eq. 2 has no simple analytical solution. Nevertheless, the differential equation can be solved if the convective term ax^2 is negligibly small. For a region very close to the membrane, where the condition $v_t \gg ax^2$ is fulfilled and assuming that the concentration of the permeable solute, c_p, reaches the value $c_{p,s}$ at the membrane surface ($x = 0$), Eq. 2 is transformed into

$$c_p(x) = \frac{J_m}{v_t} + \left(c_{p,s} - \frac{J_m}{v_t}\right)e^{-(v_t x/D_p)}. \quad (7)$$

J_m has two components. The first component is due to the permeability of the membrane to the solute, i.e., it is proportional to its transmembrane concentration gradient (Fig. 1 *b*). The second component is built up by solute molecules that are dragged by water through the pores. It does not disappear in the absence of solute gradients across the membrane (Barry and Diamond, 1984). Provided that $\Delta c_{p,s} = 0$, J_m is equal to $J_{m,t}$, the flux of cations that are dragged across the channels by the osmotic water flux (Fig. 1 *c*).

Under these conditions, cation flux adds to the water flux. The velocities of the resulting volume and water fluxes, J_v and v_t, respectively, are linked to each other by a factor of proportionality α:

$$v_t = \alpha J_v. \quad (8)$$

If the membrane conductance, G, is monitored along with v_t, it is possible to calculate the single-channel water permeability coefficient, p_f, and the number of water molecules, N, that are required to transport one ion across the channel. According to Levitt et al. (1978), J_v and the transmembrane current density, I, can be written as a linear combination of the electrical potential, $\Delta\psi$, and the osmotic pressure difference, $\Delta\pi$:

$$J_v = \frac{V_W P_f}{RT}\alpha\Delta\pi + L_{12}\Delta\psi, \quad (9)$$

$$I = L_{21}\alpha\Delta\pi + G\Delta\psi, \quad (10)$$

where L_{12} and L_{21} are cross-coefficients that are equal by Onsager's theorem. They are found if the boundary conditions 1) $\Delta\pi = 0$ and 2) $I = 0$ are subsequently applied to Eqs. 9 and 10. 1) The absence of an osmotic pressure gradient refers to electroosmotic experiments, where the number of water molecules transported per ion is simply the ratio of water and ion fluxes ($N = J_W/J_m$) (Rosenberg and Finkelstein, 1978a; Levitt et al., 1978):

$$\left(\frac{J_v}{I}\right)_{\Delta\pi=0} = \frac{J_W V_W + J_m V_c}{zFJ_m} = \frac{V_W}{zF}\left(N + \frac{V_c}{V_W}\right) = \frac{L_{12}}{G}, \quad (11)$$

where V_c is the volume change in solution when a cation passes through the membrane. 2) The second condition is fulfilled in streaming potential experiments (Rosenberg and

Finkelstein, 1978a; Levitt et al., 1978; Tripathi and Hladky, 1998):

$$\left(\frac{\Delta\psi}{\Delta\pi}\right)_{I=0} = \frac{L_{12}\alpha}{G} = -\frac{V_W}{zF}N. \quad (12)$$

From the combined Eqs. 11 and 12, the cross-coefficient is found, which, if inserted into Eq. 10, gives for $\Delta\psi = 0$

$$J_{m,t} = RT\chi c_{osm}V_w NG/z^2F^2. \quad (13)$$

Equation 13 is used to calculate N from solvent drag experiments. N must be the same when it is determined in any of three ways: electroosmosis (Eq. 11), streaming potential (Eq. 12), and solvent drag (Eq. 13).

The hydraulic permeability coefficient of a single channel, p_f, is equal to the absolute hydraulic conductivity of all channels divided by the number of channels, n. n is anticipated to be equal to the ratio of the actual membrane conductance, G, and the single-channel conductance, g (Finkelstein, 1987):

$$p_f = P_f A/n = P_{f,c}Ag/G, \quad (14)$$

where A is the membrane area. From Eqs. 5 and 14, p_f is found as

$$p_f = \frac{\Delta v}{V_w\chi c_{osm}}\frac{g}{G}A. \quad (15)$$

c_{osm} is not identical to the osmolyte bulk concentration, $c_{osm,b}$. Because c_{osm} cannot be measured directly, it is derived from the difference in the near-membrane and bulk concentrations of the impermeable cation, denoted as $c_{i,s}$ and $c_{i,b}$, respectively. Therefore, Eqs. 1 and 3 are combined into the expression

$$v = -D_{osm}(c_{osm} - c_{osm,b})/\delta_{osm}c_{osm} = -D_i(c_{i,s} - c_{i,b})/\delta_i c_{i,s}. \quad (16)$$

Because the ratio of the USL thicknesses of two different substances is equal to the third root of the ratio of the respective diffusion coefficients (Pohl et al., 1998),

$$\frac{\delta_{osm}}{\delta_i} = \sqrt[3]{\frac{D_{osm}}{D_i}}, \quad (17)$$

Eq. 11 can be transformed into

$$\sqrt[3]{\frac{D_i^2}{D_{osm}^2}}\left[1 - \frac{c_{i,b}}{c_{i,s}}\right] = 1 - \frac{c_{osm,b}}{c_{osm}}. \quad (18)$$

MATERIALS AND METHODS

Membranes

Planar bilayer lipid membranes were formed (Mueller et al., 1963) from diphytanoylphosphatidylcholine (DPhPC) (Avanti Polar Lipids, Alabaster, AL) dissolved at 20 mg/ml in *n*-decane (Merck, Darmstadt, Germany). They were spread across a circular hole (0.8 or 1.1 mm in diameter) in a diaphragm separating two aqueous phases of a polytetrafluorethylene chamber. The aqueous salt solutions (Merck) were buffered with 10 mM Tris (Fluka, Buchs, Switzerland) or 10 mM morpholinoethanesulfonic acid (MES) (Boehringer-Mannheim, Mannheim, Germany). They were agitated by magnetic stirrer bars. Gramicidin (Sigma, Dreisenhofen, Germany) was added to the aqueous phase from a stock solution in ethanol.

Osmotic gradients were imposed by urea (Laborchemie Apolda, Apolda, Germany) and sodium or choline chloride. These osmolytes have a negligible effect on bulk viscosity. Therefore, it is assumed that they do not alter the thickness δ of the USLs (Pedley, 1983). The permeabilities of the lipid bilayer for the salts and for urea are much lower than the water permeability (Finkelstein, 1976). A membrane doped with gramicidin is permeable for sodium and potassium ions but not for urea (Finkelstein, 1987). Consequently, the latter may be treated as a nonpenetrating solute that is completely reflected by the membrane.

Concentration profiles

In the immediate vicinity of the membrane, the spatial distributions of two different ions were monitored simultaneously. Therefore, a double-barreled microelectrode and a reference electrode were placed at the *trans* side (unless otherwise stated) of the bilayer membrane (Fig. 1 *a*). The ion sensitivity was achieved by filling both glass barrels with ionophore cocktails (Fluka) according to the procedure described by Amman (1986). Their tips had a diameter of ~1–2 μm.

The experimental arrangement was similar to the one described previously (Antonenko et al., 1993; Pohl et al., 1993). Voltage sampling was performed with two electrometers (model 617; Keithley Instruments, Cleveland, OH) connected via an IEEE interface to a personal computer. The double-barreled microelectrode was moved perpendicular to the surface of the bilayer membrane by a hydraulic microdrive manipulator (Narishige, Tokyo, Japan). The touching of the membrane was indicated by a steep potential change (Antonenko and Bulychev, 1991). From the known velocity of the electrode motion (1–2 μm s^{-1}), the position of the microsensor relative to the membrane could be determined at any instant of the experiment. Artifacts due to the slow electrode movement are unlikely because the response of the electrode potential to concentration changes occurred comparatively fast, i.e., the 90% rise time was below 0.6 s. Nevertheless, possible effects of time resolution or distortion of the USLs were tested by making measurements while moving the microelectrode toward and away from the bilayer. Because no hysteresis was found, it can be assumed that an electrode of appropriate time resolution was driven without any effect on the USLs. The accuracy of the distance measurements was estimated to be ± 8 μm.

Current and conductance measurements

Under short-circuited conditions, a transmembrane current through cation-selective membranes can be observed. During osmosis, it persists even if no transmembrane potential or concentration gradient is imposed. To monitor the current, Ag/AgCl pellets that were connected to a picoampermeter (model 428; Keihley Instruments) were immersed in the bathing buffer solutions on both sides of the membrane. The amplified signal was visualized with a voltmeter.

Membrane conductance was measured just before and just after the volume flux measurement. Two pairs of electrodes were exploited. The first pair of Ag/AgCl pellets was used to monitor a current step. A 1-kHz square-wave input voltage (source: model 33120A; Hewlett-Packard, Loveland, CO) was applied to the membrane. The output signal was first amplified by a current amplifier (model 428; Keihley Instruments) and then transferred to an oscilloscope (model TDS 340; Tektronix, Wilsonville, OR). Through the second pair of pellets, the resulting potential difference was recorded with an operational amplifier (AD549; Analog Devices, Norwood, MA) and displayed on the second channel of the oscilloscope.

RESULTS

On both sides of a planar membrane calcium and sodium concentration profiles were monitored simultaneously with the use of a double-barreled microelectrode (Fig. 2). The velocity of the transmembrane volume flux that was induced by the addition of 0.3 M choline chloride at the *cis* side was equal to 1.2 μmol s^{-1} cm^{-2}. The volume flow swept solute away from the membrane in the *cis*-USL and swept solute toward the membrane in the *trans*-USL. Addition of gramicidin greatly increased these polarization effects. According to Eqs. 3 and 6, the water flux obtained from the calcium concentration distribution on both sides of the membrane was equal to 17 μmol s^{-1} cm^{-2}. Because the sodium profiles gave the same value, it was concluded that no transmembrane sodium flux occurred. This result was expected because electroneutrality must be maintained, i.e., in an open circuit there can be no net cation flux through membranes containing only cation-selective channels (Dani and Levitt, 1981).

The same result was obtained when the impermeable osmolyte choline chloride was substituted for sodium chloride (Fig. 3). From the representative calcium and sodium concentration profiles recorded with double-barreled microelectrodes at the *trans* side of a bilayer membrane doped with gramicidin, a volume flux of 8 μmol s^{-1} cm^{-2} was calculated. Also in this case, no transmembrane sodium flux was observed. Gramicidin provoked only an increase in the water flux, which in the channel free membrane was equal to 1.5 μmol s^{-1} cm^{-2}.

In contrast to the effects observed in an open-circuited situation, channel insertion into a short-circuited membrane was accompanied by a decrease in the osmotically induced near-membrane polarization of the permeable cation (Fig. 4). The transmembrane movement of the monovalent ion was responsible for this phenomenon. An increasing number of gramicidin channels rendered the membrane more and more permeable. As a consequence, the number of ions that were able to diffuse along their transbilayer concentration gradient increased, and at a very large channel density, the concentration gradients of the monovalent cations dissipated (Fig. 4). At the same time, the increase in the transmembrane volume flow resulted in an increasing polarization of the impermeable solute. The additional water permeability that is introduced by the porous pathway was calculated from the Ca^{2+} concentration profiles. Therefore, v_t was obtained by fitting the parametric Eq. 3 to the experimental data set. For the minimization of the least-square residuals, the program SigmaPlot was used. From a comparison with the unmodified membrane, Δv was deduced. According to Eqs. 5 and 15, $P_{f,c}$ and p_f were then obtained. The corresponding increase in the electric conductance is plotted in Fig. 5. From the slopes of the linear regressions in 10 and 1 mM NaCl, single-channel hydraulic permeability coefficients of 1.7 and 1.4 $\times$ 10^{-14} cm^3 s^{-1} were found, respectively. For the calculations according to Eq. 15, the single-channel conductance of 5.1 pS measured

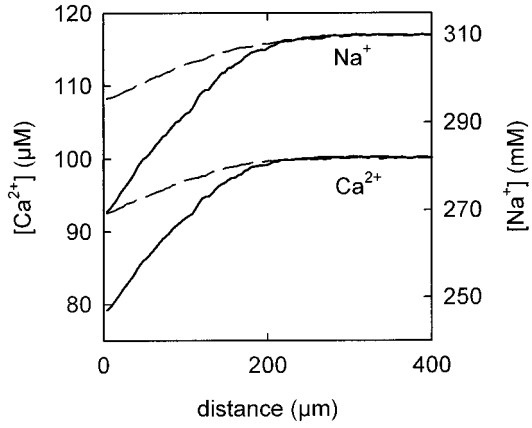

FIGURE 3 Representative calcium and sodium concentration profiles at the *trans* side of a bilayer membrane. Because of the NaCl concentration gradient (10 mM at the *cis* and 310 mM at the *trans* side) a transmembrane volume flux was induced. It increased from 1.5 μmol s^{-1} cm^{-2} to 8 μmol s^{-1} cm^{-2} after the addition of 0.5 μg/ml gramicidin. Under open-circuited conditions, a transmembrane Na^+ flux was not observed. The bulk solution contained 10 mM Tris, 10 mM MES, 0.1 mM $CaCl_2$.

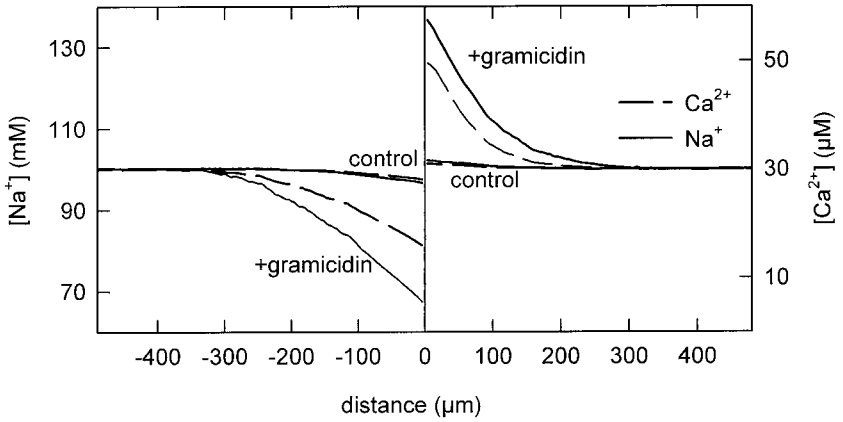

FIGURE 2 Representative calcium and sodium concentration profiles under open-circuited conditions. Because of the addition of 0.3 M choline chloride at the *cis* side, a transmembrane volume flux is induced (1.2 μmol s^{-1} cm^{-2}). It sweeps solute away from the membrane in the *trans* unstirred layer (USL) and sweeps solute toward the membrane in the *cis* USL (control). The addition of gramicidin (final concentration 3 μg/ml) substantially increases these polarization effects. No transmembrane sodium flux is detected. The water flux obtained from the calcium and the sodium profiles on either side of the membrane is equal to 17 μmol s^{-1} cm^{-2}. The buffer solutions contained 10 mM Tris and MES, 100 mM NaCl, and 30 μM Ca^{2+}. pH was 7.5.

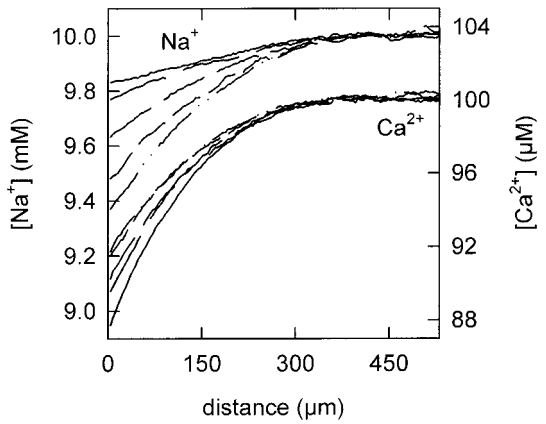

FIGURE 4 Osmosis-mediated dilution of two different solutes in the membrane vicinity under short-circuited conditions. The dashed-dotted line denotes profiles near the unmodified bilayer. After channel insertion, the polarization of the gramicidin-impermeable Ca^{2+} increases, whereas the polarization of the permeable Na^+ decreases. The augmentation of the gramicidin concentration is indicated by the length of the dashes, reaching a maximum with the spline line (20 ng/ml). The solutions contained 10 mM Tris and 150 mM choline chloride. The pH was 8.4. To the *trans* compartment 1 M urea was also added.

with DPhPC membranes in 100 mM NaCl (Andersen, 1983; Busath et al., 1998) was corrected for the lower electrolyte concentration used in our experiments according to the results of Neher et al. (1978). For 10 and 1 mM NaCl, a single-channel conductance of 0.7 and 0.11 pS, respectively, was assumed.

Along with the gramicidin hydraulic conductivity, the competition of water and ion flux was explored. The sodium

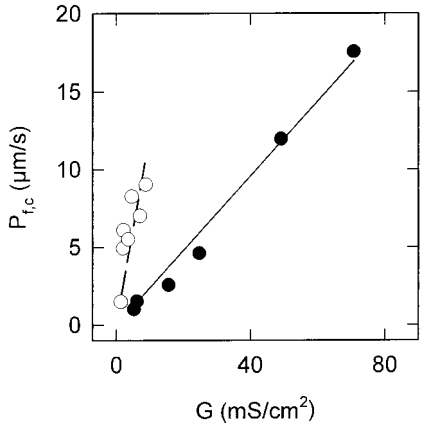

FIGURE 5 Determination of the single-pore water permeability coefficient. From two additional runs of the experiment shown in Fig. 4 and three similar experiments in which the sodium concentration was lowered to 1 mM, the calcium concentration profiles (NaCl bulk concentrations: 1 mM, ○; 10 mM, ●) were used to calculate the gramicidin-mediated increase in the hydraulic membrane conductance $P_{f,c}$. From the membrane conductance, G, measured and the published single-channel conductance, the single-pore water permeability coefficient was calculated to be 1.4×10^{-14} cm^3 s^{-1} (○) or 1.7×10^{-14} cm^3 s^{-1} (●).

flux density in the first experiment of Fig. 6 equals 26 pmol cm^{-2} s^{-1}. It was determined by fitting the parametric Eq. 7 to the experimental data set in the interval $0 \le x \le 50$ μm. In this region, $ax^2 \ll v$, as revealed by the analysis of the Ca^{2+} concentration distribution with the help of Eq. 3. In the named interval, it was impossible to find all three parameters, J_m, v_t, and $c_{p,s}$ with sufficient accuracy. A satisfying fit to Eq. 7 was achieved only when v_t was fixed to the value calculated from the concentration distribution of the impermeable solute. For the two remaining parameters, J_m and $c_{p,s}$, the least-squares minimization gave a standard deviation of no more than 5% and a dependency of better than 98%. The Na^+ flux determined according to this procedure for the second experiment in Fig. 6 was equal to 16 pmol cm^{-2} s^{-1}. The flux values for the two Na^+ profiles were different because in the second experiment, solely true solvent drag was responsible for the transmembrane ion flux. Both true and pseudo-solvent drag contributed to the distribution in the first experiment.

The only differences in the experimental conditions for the first and second experiments in Fig. 6 were, respectively, the presence and the absence of a transmembrane sodium concentration gradient. To compensate for the flow-induced decrease in the near-membrane sodium concentration (*curve 1*) on one side of the membrane and the equally large sodium concentration increase on the opposite side of the membrane, the salt concentration in the hypertonic com-

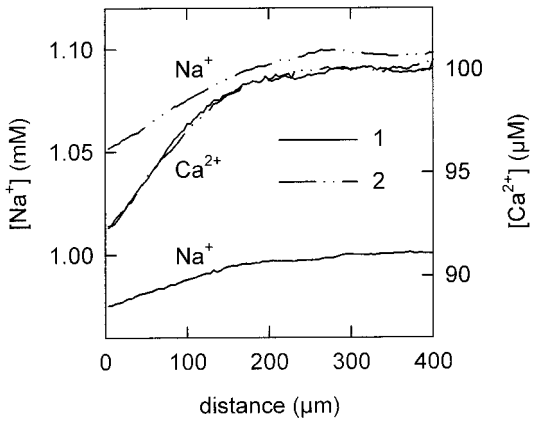

FIGURE 6 Visualization of solvent drag. Under short-circuited conditions (experiment 1) potassium (1 mM in the *cis* and *trans* bulk solutions) is dragged by the osmotic water flow across gramicidin channels and flows along its concentration gradient (*spline line*). The latter is zero after the bulk concentration of NaCl on the *trans* side had been augmented to 1.1 mM (experiment 2). In this situation only true solvent drag occurs, which accounts for a sodium flux density of only 16 pmol cm^{-2} s^{-1} (*dashed line*), in contrast to the initially measured 26 pmol cm^{-2} s^{-1} (*spline line*). From simultaneous current measurements, the flux density in the case of true solvent drag was found to be equal to 13 pmol cm^{-2} s^{-1}. With respect to the conductivity of 0.74 mS cm^{-2}, the number of water molecules moving along with one cation is calculated to be 5.2 or 4.4, depending on whether the flux value based on microelectrode or current measurements, respectively, was chosen.

partment was enhanced by NaCl titration (compare Fig. 1 *c*). The addition of only 0.1 mM NaCl was sufficient to establish a situation in which the near-membrane NaCl concentrations on the two sides of the bilayer were equal to each other (*curve 2*). In Fig. 6 only the hyperosmotic concentration profile was shown. The symmetry of the experimental system justified the assumption that the absolute concentration changes on the two sides of the membrane were identical. At least for small concentration changes, the difference between the surface and bulk concentrations is shown to differ only in sign for the *cis* and *trans* USLs (Pohl et al., 1997). During the titration procedure, the osmotic gradient generated by 1 M urea remained unchanged.

In parallel, the current density, I, was measured. I is related to J_m by

$$I = zFJ_m \tag{19}$$

According to Eq. 19, a flux of 13 pmol cm^{-2} s^{-1} was found for experiment 2 in Fig. 6. Considering that the current measurements returned an average for the flux over the whole membrane area, whereas the microelectrode measurements reflected the maximum flux in the center of the membrane, it had to be acknowledged that the two methods were in perfect agreement with each other.

The number of water molecules that are moving along with one sodium ion was calculated (Eq. 13), taking into account the membrane conductivity and correcting the osmolyte concentration for volume flow dilution (Eq. 18). In the particular experiment described above (Fig. 6), N was equal to 5.2 or 4.4, depending on whether the flux value based on microelectrode or current measurements, respectively, was chosen. From the current measured in five additional runs of the experiment (Fig. 6), N was calculated to be equal to 4.8 $\pm$ 0.7. Preference was given to the flux value based on current measurements because the systematic error of this method was smaller. It did not exceed 2% because in all short-circuited experiments reported here, the access resistance (electrode resistance) was at least two orders of magnitude lower than the membrane resistance. In contrast, a small error in the determination of v_t with the microelectrode approach resulted in a comparatively large error of J_m because v_t was used in the fit procedure chosen (compare Eq. 7).

Similar experiments were carried out with potassium ions. Fig. 7 shows representative K^+ and Ca^{2+} profiles measured under short-circuited conditions in the immediate vicinity of a bilayer membrane. As in the case of Na^+ ions, the polarization of K^+ ions depended on the transmembrane K^+ concentration difference. While the latter was minimized by adding KCl to the hypertonic compartment, the former increased. In the absence of the transmembrane K^+ concentration gradient (*curve 2*), the K^+ flux across the membrane was equal to 86 pmol s^{-1} cm^{-2}. In this experiment, solvent drag was responsible for 45% of the total potassium ion flux measured initially (*curve 1*). With identical K^+ bulk concentrations on both sides of the bilayer, J_m equaled 0.19 nmol s^{-1} cm^{-2} (*curve 1*). The amount of potassium ions that are dragged through the gramicidin channels depended on the volume flow velocity. With an increase in the osmotic gradient (*curves 3* and *4*), the water flux and, consequently, the cation flux increased. According to Eq. 13, J_m normalized by the channel density was anticipated to be proportional to the osmotic pressure. As seen from the inset of Fig. 7, the expectation is satisfied by the experiment. From the slope, the number of water molecules that were moving along with one K^+ was calculated. In that particular experiment, N was equal to 4.3. Five additional experiments gave an average of 4.6 $\pm$ 0.6.

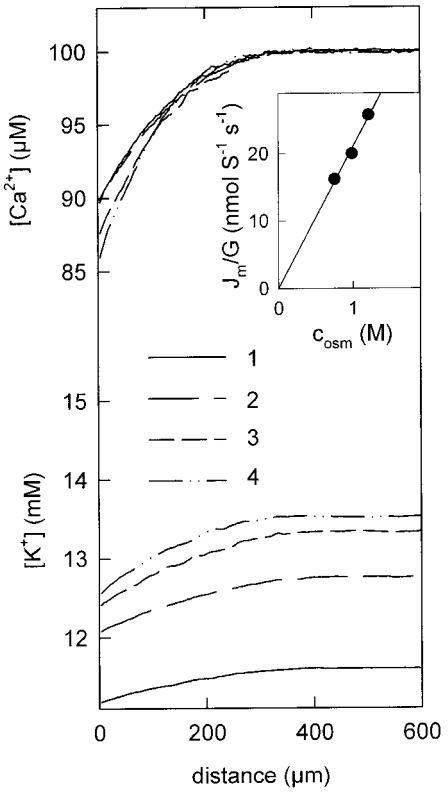

FIGURE 7 Number of water molecules transported along with one potassium ion. The experiment from Fig. 6 was repeated, substituting Na^+ for 11.6 mM KCl in the *cis* and *trans* bulk solutions. Pseudo-solvent drag that was observed under these conditions (experiment 1) disappeared after the *trans* KCl concentration was augmented to 12.8, 13.3, and 13.5 mM at 1 (experiment 2), 1.3 (experiment 3), and 1.6 (experiment 4) M urea. Current measurements gave a K^+ flux across the membrane that was equal to 0.19 nmol s^{-1} cm^{-2} (*1*) in the presence of a transmembrane K^+-concentration gradient and to 86 pmol s^{-1} cm^{-2} in its absence (*2*). N is the number of potassium ions that are dragged through the gramicidin channels; when corrected for membrane conductance, G, J_m is proportional to the effective osmotic gradient c_{osm} (see *inset*). N was calculated from the slope to be 4.3.

DISCUSSION

In the presence of channels that allow volume flow, the microelectrode technique permits us to measure the compe-

tition of solvent and solute fluxes across a membrane. Moreover, the two components of the solute flux, true solvent drag and pseudo-solvent drag, can be discriminated. The former is shown to persist even when solute concentrations at opposite faces of the membrane are identical (Figs. 6 and 7). In view of frictional interactions between solute and water traversing the membrane in the same channels, the phenomenon was predicted (Barry and Diamond, 1984, and references therein). Because of the accompanying pseudo-solvent drag, direct experimental visualization of true solvent drag, however, is difficult to accomplish (Finkelstein, 1987). Because pseudo-solvent drag is due to the permeability of the channel to the solute, it is negligible if the solute gradient across the membrane is also negligible. The latter situation was shown to be attainable when the near-membrane concentration is controlled by microelectrodes. The flux measured under such conditions is roughly one-half of the sodium or potassium flux obtained when no correction for volume flow-induced concentration changes is made, i.e., both true and pseudo-solvent drag account for roughly one-half of the total cation flux across gramicidin channels under our conditions (Figs. 6 and 7).

The osmotic water permeability coefficient per gramicidin channel in the absence of cations was found to be $1.6 \pm 0.3 \times 10^{-14}$ cm^3 s^{-1}. This value is significantly smaller than 6×10^{-14} cm^3 s^{-1} (Dani and Levitt, 1981) and 9×10^{-14} cm^3 s^{-1} (Wang et al., 1995) reported for membranes made from glycerol monoolein but close to the value 9.6×10^{-15} cm^3 s^{-1} obtained for membranes made from phosphatidylethanolamine (Rosenberg and Finkelstein, 1978b). The latter value is based on underestimated values for single gramicidin channel conductance and membrane water permeability. The authors have obtained g in 10 mM NaCl by simple division of g published for 100 mM. Because the single-channel conductance does not depend linearly on the solute concentration (Hladky and Haydon, 1984), an underestimation of 40% may be suggested (Dani and Levitt, 1981). The underestimation of P_f results from water flow-mediated osmolyte dilution in the immediate membrane vicinity (i.e., an overestimation of c_{osm} in Eq. 4) that was neglected (for our correction see Eqs. 16–18). When corrected, Rosenberg and Finkelstein's value for the hydraulic conductivity per pore comes into close agreement with ours but both remains well below the one found for glycerol monoolein. In a simulation study of a gramicidin/lipid bilayer system, the large discrepancy in p_f measured with glycerolmonooleate and phospholipid bilayers was attributed to a different hydration environment for water just outside the channel mouth in the two environments (Chiu et al., 1999).

From ion flux measurements carried out in the absence of a transmembrane cation concentration gradient, the number of water molecules that were moving along with one Na^+ or one K^+ was calculated to be equal to 4.8 ± 0.8 and 4.6 ± 0.6, respectively (Figs. 6 and 7). Our value for sodium does not differ significantly from the published value of 5.3 that was found on the basis of flux measurements (Rosenberg and Finkelstein, 1978b). In their paper, the authors have obtained N as the ratio of the osmotic and diffusion permeabilities (P_f and P_d). In part, the already discussed underestimation of P_f was compensated by an underestimation of P_d. Rosenberg and Finkelstein have used an improper correction for unstirred layer effects. The membrane permeability P_d of the water radioisotope THO was calculated from the observed permeability, $P_{observed}$ ($1/P_{observed} = \delta_{water}/D + 1/P_d$), and the USL thickness that was measured for a butanol tracer. Thereby, they neglected the fact that δ ($\delta_{THO} = 0.75\delta_{butanol}$) depends on the diffusion coefficient (Pohl et al., 1998), a phenomenon that at that time was described only in a theoretical study (Levich, 1962).

In an independent approach N was found in an open-circuited situation. Streaming potential measurements for K^+ gave 6.6 (Tripathi and Hladky, 1998), 6.5 (Rosenberg and Finkelstein, 1978a), and 7.1 (Levitt et al., 1978). The values for Na^+ were equal to 7.1 (Tripathi and Hladky, 1998), 6.5 (Rosenberg and Finkelstein, 1978a), and 9 (Levitt, 1984). This approach also requires corrections for USL effects. The most accurate method currently available for this purpose is microelectrode measurement in the immediate membrane vicinity. Nevertheless, microelectrode aided streaming potential measurements may also reveal an N that is overestimated by 1 because of the nonideality of the electrodes (Tripathi and Hladky, 1998). Consequently, the number of water molecules (five molecules) that we have found to be in a row with one cation in the gramicidin channel appears to be in reasonable agreement with previously published numbers.

To summarize: the microelectrode technique is shown to be a very elegant tool for demonstrating true solvent drag and for monitoring the competition of ion and water fluxes across membranes. In a single experiment, the hydraulic membrane permeability, the single-pore water permeability coefficient, and the number of water molecules per ion in single-file transport can be determined. The main advantage of this method is that instead of making corrections for USL effects, one explores the phenomena related to the diffusion boundary layer for the measurements. Flux and permeability data are deduced from concentration gradients within the USLs that arise only because of diffusion limitations. The approach is suitable not only for the investigation of model channels in planar membranes; it applies also to reconstituted natural water channels. It is not even restricted to microelectrodes. Instead of measuring the concentration profile of ions, one can monitor the concentration distribution of a fluorescence dye adjacent to cells to estimate flux (Phillips et al., 1999) and permeability (Kovbasnjuk et al., 1998) parameters.

This work was supported by the Deutsche Forschungsgemeinschaft, Germany (Po 533/2-2).

REFERENCES

Amman, D. 1986. Ion-Selective Microelectrodes. Principles, Design and Application. Springer-Verlag, Berlin.

Andersen, O. S. 1983. Ion movement through gramicidin A channels. Single-channel measurements at very high potentials. *Biophys. J.* 41: 119–133.

Andreoli, T. E., J. A. Schafer, and S. L. Troutman. 1971. Coupling of solute and solvent flows in porous lipid bilayer membranes. *J. Gen. Physiol.* 57:479–493.

Antonenko, Y. N., and A. A. Bulychev. 1991. Measurements of local pH changes near bilayer lipid membrane by means of a pH microelectrode and a protonophore-dependent membrane potential—comparison of the methods. *Biochim. Biophys. Acta.* 1070:279–282.

Antonenko, Y. N., G. A. Denisov, and P. Pohl. 1993. Weak acid transport across bilayer lipid membrane in the presence of buffers—theoretical and experimental pH profiles in the unstirred layers. *Biophys. J.* 64: 1701–1710.

Antonenko, Y. N., P. Pohl, and G. A. Denisov. 1997. Permeation of ammonia across bilayer lipid membranes studied by ammonium ion selective microelectrodes. *Biophys. J.* 72:2187–2195.

Barry, P. H., and J. M. Diamond. 1984. Effects of unstirred layers on membrane phenomena. *Physiol. Rev.* 64:763–872.

Busath, D. D., C. D. Thulin, R. W. Hendershot, L. R. Phillips, P. Maughan, C. D. Cole, N. C. Bingham, S. Morrison, L. C. Baird, R. J. Hendershot, M. Cotten, and T. A. Cross. 1998. Noncontact dipole effects on channel permeation. I. Experiments with (5F-indole)Trp(13) gramicidin A channels. *Biophys. J.* 75:2830–2844.

Chiu, S. W., S. Subramaniam, and E. Jakobsson. 1999. Simulation study of a gramicidin/lipid bilayer system in excess water and lipid. II. Rates and mechanisms of water transport. *Biophys. J.* 76:1939–1950.

Dainty, J. 1963. Water relations in plant cells. *Adv. Bot. Res.* 1:279–326.

Dani, J., and D. G. Levitt. 1981. Binding constants of Li^+, K^+, and Tl^+ in the gramicidin channel determined from water permeability measurements. *Biophys. J.* 35:485–499.

Deamer, D. W., and J. Bramhall. 1986. Permeability of lipid bilayers to water and ionic solutes. *Chem. Phys. Lipids.* 40:167–188.

Fettiplace, R., and D. A. Haydon. 1980. Water permeability of lipid membranes. *Physiol. Rev.* 60:510–550.

Finkelstein, A. 1976. Water and nonelectrolyte permeability of lipid bilayer membranes. *J. Gen. Physiol.* 68:127–135.

Finkelstein, A. 1987. Water Movement through Lipid Bilayers, Pores, and Plasma Membranes. Wiley and Sons, New York.

Finkelstein, A., and O. S. Andersen. 1981. The gramicidin A channel: a review of its permeability characteristics with special reference to the single-file aspect of transport. *J. Membr. Biol.* 59:155–171.

Ge, M., and J. H. Freed. 1999. Electron-spin resonance study of aggregation of gramicidin in dipalmitoylphosphatidylcholine bilayers and hydrophobic mismatch. *Biophys. J.* 76:264–280.

Hanai, T., and D. A. Haydon. 1966. The permeability to water of bimolecular lipid membranes. *J. Theor. Biol.* 11:370–382.

Hill, A. E. 1995. Osmotic flow in membrane pores. *Int. Rev. Cytol.* 163:1–42.

Hladky, S. B., and D. A. Haydon. 1984. Ion movements in gramicidin channels. *Curr. Top. Membr. Transp.* 21:327–372.

Jansen, M., and A. Blume. 1995. A comparative study of diffusive and osmotic water permeation across bilayers composed of phospholipids with different head groups and fatty acyl chains. *Biophys. J.* 68: 997–1008.

Kovbasnjuk, O. N., J. P. Leader, A. M. Weinstein, and K. R. Spring. 1998. Water does not flow across the tight junctions of MDCK cell epithelium. *Proc. Natl. Acad. Sci. USA.* 95:6526–6530.

Levich, V. G. 1962. Physicochemical Hydrodynamics. Prentice-Hall, Englewood Cliffs, NJ.

Levitt, D. G. 1984. Kinetics of movements in gramicidin channels. *Curr. Top. Membr. Transp.* 21:181–197.

Levitt, D. G., S. R. Elias, and J. M. Hautman. 1978. Number of water molecules coupled to the transport of sodium, potassium and hydrogen ions via gramicidin, nonactin or valinomycin. *Biochim. Biophys. Acta.* 512:436–451.

Mueller, P., D. O. Rudin, H. T. Tien, and W. C. Wescott. 1963. Methods for the formation of single bimolecular lipid membranes in aqueous solution. *J. Phys. Chem.* 67:534–535.

Nakahari, T., H. Yoshida, and Y. Imai. 1996. Transepithelial fluid shift generated by osmolarity gradients in unstimulated perfused rat submandibular glands. *Exp. Physiol.* 81:767–779.

Neher, E., J. Sandblom, and G. Eisenman. 1978. Ionic selectivity, saturation, and block in gramicidin A channels. II. Saturation behavior of single channel conductances and evidence for the existence of multiple binding sites in the channel. *J. Membr. Biol.* 40:97–116.

Pappenheimer, J. R., C. E. Dahl, M. L. Karnovsky, and J. E. Maggio. 1994. Intestinal absorption and excretion of octapeptides composed of D amino acids. *Proc. Natl. Acad. Sci. USA.* 91:1942–1945.

Pedley, T. J. 1983. Calculation of unstirred layer thickness in membrane transport experiments: a survey. *Q. Rev. Biophys.* 16:115–150.

Phillips, J. E., L. B. Wong, and D. B. Yeates. 1999. Bidirectional transepithelial water transport: measurement and governing mechanisms. *Biophys. J.* 76:869–877.

Pohl, P., Y. N. Antonenko, and E. H. Rosenfeld. 1993. Effect of ultrasound on the pH profiles in the unstirred layers near planar bilayer lipid membranes measured by microelectrodes. *Biochim. Biophys. Acta.* 1152:155–160.

Pohl, P., S. M. Saparov, and Y. N. Antonenko. 1997. The effect of a transmembrane osmotic flux on the ion concentration distribution in the immediate membrane vicinity measured by microelectrodes. *Biophys. J.* 72:1711–1718.

Pohl, P., S. M. Saparov, and Y. N. Antonenko. 1998. The size of the unstirred layer as a function of the solute diffusion coefficient. *Biophys. J.* 75:1403–1409.

Rippe, B., and B. Haraldsson. 1994. Transport of macromolecules across microvascular walls: the two-pore theory. *Physiol. Rev.* 74:163–219.

Rosenberg, P. A., and A. Finkelstein. 1978a. Interactions of ions and water in gramicidin A channels: streaming potentials across lipid bilayer membrane. *J. Gen. Physiol.* 72:327–340.

Rosenberg, P. A., and A. Finkelstein. 1978b. Water permeability of gramicidin A-treated lipid bilayer membranes. *J. Gen. Physiol.* 72:341–350.

Rutledge, J. C., F. E. Curry, P. Blanche, and R. M. Krauss. 1995. Solvent drag of LDL across mammalian endothelial barriers with increased permeability. *Am. J. Physiol.* 268:H1982–H1991.

Schlichting, H., and K. Gersten. 1997. Grenzschicht-Theorie. Springer-Verlag, Berlin.

Tripathi, S., and S. B. Hladky. 1998. Streaming potentials in gramicidin channels measured with ion-selective microelectrodes. *Biophys. J.* 74: 2912–2917.

Wang, K. W., S. Tripathi, and S. B. Hladky. 1995. Ion binding constants for gramicidin a obtained from water permeability measurements. *J. Membr. Biol.* 143:247–257.

Wilson, R. W., M. Wareing, and R. Green. 1997. The role of active transport in potassium reabsorption in the proximal convoluted tubule of the anaesthetized rat. *J. Physiol. (Lond.).* 500:155–164.